Available online at www.sciencedirect.com
SCIENCE DIRECT
Catalysis Today 107–108 (2005) 377–387
CATALYSIS TODAY
www.elsevier.com/locate/cattod

Molten carbonate fuel cell cathodes: Improvement of the electrocatalytic activity

M.J. Escudero [a,*], T. Rodrigo [b], L. Daza [a,b]

[a] Dpto. Energía, CIEMAT, Av. Complutense 22, 28040 Madrid, Spain
[b] Instituto de Catálisis y Petroleoquímica, CSIC, Campus Cantoblanco, 28049 Madrid, Spain

Available online 19 September 2005

Abstract

The purpose of this work is to improve the electrocatalytic activity of Li–Ni mixed oxides by the addition of rare earth oxides (cerium or lanthanum). The influence of cerium and lanthanum on the electrocatalytic activity of these compounds was investigated by means of electrochemical impedance spectroscopy (EIS). The stability of these compounds was studied in a mixture of 62% lithium carbonate and 38% potassium carbonate at high temperature under an atmosphere rich in carbon dioxide to accelerate their dissolution. The morphology and the crystalline structure of the samples were not affected by the incorporation of cerium or lanthanum. The samples impregnated with CeO_2 or La_2O_3 showed lower resistance to charger-transfer processes than the sample without earth rare oxides. Both cerium and lanthanum improved the charger-transfer processes for oxygen reduction in an atmosphere rich in carbon dioxide. The reason may be due to cerium oxide acting as oxygen donor, and lanthanum oxide capturing CO_2, and the partial pressure of carbon dioxide on the surface of electrode.

Keywords: Lithium nickel oxide; MCFC; Cathode; Electrochemical impedance spectroscopy; Fuel cell

1. Introduction

One of the problems limiting the lifetime of the molten carbonate fuel cells (MCFC) is the slow dissolution of cathode material NiO into the electrolyte. There are three approaches to overcome this problem: the development of alternative cathode materials, the modifications of NiO with stable materials or with high lithium content and the modifications of the electrolyte with additives that stabilize the cathode dissolution.

With regard to the first approach, alternative cathode materials, such as $LiCoO_2$, $LiFeO_2$ and Li_2MnO_3, have been investigated [1–5]. $LiCoO_2$ was considered as the most promising due to its lower solubility in molten carbonate and its comparable electrochemical performance with NiO. However, problems in scale-up of the electrode area and relatively high cost of cobalt restricted the practical utilization of $LiCoO_2$ cathode [6].

Concerning the second approach, NiO has been modified mostly with $LiCoO_2$ [5–7], but CeO_2 [8], Nb_2O_5 [9], $LiFeO_2$ [10] and TiO_2 [11] have also been studied. $Li_xNi_{1-x}O$ with high lithium content ($x > 0.2$) showed a relatively lower rate than the cathodes with lower lithium content ($0.02 < x < 0.05$) obtained with the in situ oxidized and lithiated NiO [12].

About the third approach, the effect of the addition of alkaline earth oxide to the NiO cathode, such as MgO, CaO, SrO, BaO, SnO_2 and La_2O_3, has been investigated in various alkali carbonate electrolyte [13,14]. These alkaline earth oxides contained in the cathodes are dissolved into the electrolyte under the cell operation conditions. The dissolution of alkaline earth oxide increases the basicity of the electrolyte and then the solubility of NiO decreases.

Previous works conducted by the authors demonstrated that the incorporation of less than 1.0 wt.% of CeO_2 [15] or La_2O_3 [16] into the cathode material decreased the nickel dissolution and $Li_xNi_{1-x}O$ ($0.3 < x < 0.5$) prepared by ex situ lithiation has higher stability that the NiO in molten carbonate [17]. On the basis of these investigations novel cathodes materials with high lithium content ($x = 0.4$) were

* Corresponding author. Tel.: +34 913466622; fax: +34 913466269.
E-mail address: m.escudero@ciemat.es (M.J. Escudero).

0920-5861/$ – see front matter © 2005 Elsevier B.V. All rights reserved.
doi:10.1016/j.cattod.2005.07.097

Nomenclature

j	$\sqrt{1}$
C	capacitance
L	effective length or penetration depth
R	resistance
R_e	electrolyte resistance
R_p	pore resistance
Z	complex impedance
Z_m	contact impedance
Z_1	interface impedance
Z_0	intrinsic impedance
Z_{TL}	impedance of the reacting volume
α	degree of the dispersion of the time constant
ω	angular frequency

prepared by ex situ lithiathing of NiO, with and without cerium or lanthanum impregnation. In this study, we have examined the effect of cerium and lanthanum on the stability and the electrocatalytic activity for oxygen reduction of these compounds in molten carbonate at 650 °C.

All samples were examined by inductive coupled plasma atomic emission spectroscopy (ICP-AES), scanning electron microscopy (SEM) and X-ray diffraction (XRD) before and after their stability test in carbonate melt at 650 °C for 200 h. For comparison, the NiO was also tested under the same operation conditions. The impedance measurements as a function of partial pressure of oxygen (pO_2) and partial pressure of carbon dioxide (pCO_2) were carried out to investigate the electrocatalytic activity for oxygen reduction at novel cathode materials.

2. Experimental

2.1. Preparation of the samples

Three different samples of lithium nickel oxides were synthesized with a lithium atomic fraction of 0.4 by a solid-state reaction. The first one, labeled as LN, was prepared without rare earth oxides, and the other two samples were prepared containing 0.5% CeO_2 or 0.5% La_2O_3, labeled as LNCe and LNLa, respectively.

The sample LN was prepared by mixing nickel powder with an aqueous solution of Li_2CO_3. For the LNCe and LNLa samples, an aqueous solution of cerium nitrate or lanthanum nitrate was added, respectively, to a Li_2CO_3 solution. Precursor samples were pressed into pellets at 20 T m cm^{-2} 2 for 5 min. The pellets were then calcined at 800 °C.

2.2. Stability tests

The test cell was an alumina crucible contained in a covered stainless steel reactor. The cover of the reactor was adapted to hold a thermocouple and gas inlet/outlet. Each sample with a surface of 5 cm^2 was introduced inside the

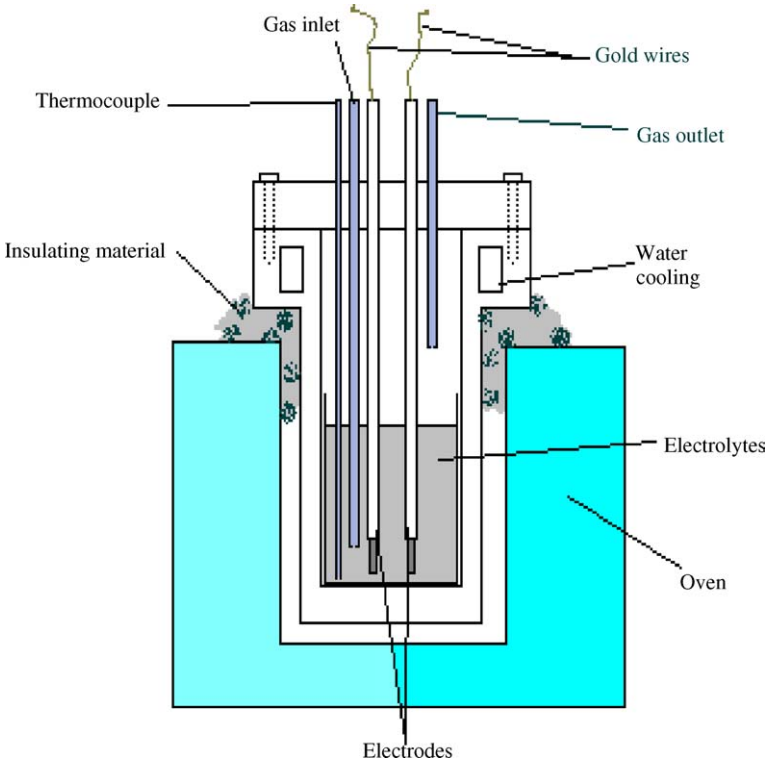

Fig. 1. Schematic of the cell used in the electrochemical test.

alumina crucible containing 75 g of molten carbonate (Li_2CO_3:K_2CO_3 = 62:38) at 650 °C during 200 h under an atmosphere with high content of carbon dioxide (CO_2:O_2 4:1), in order to accelerate the cathode dissolution and evaluate the effect of the addition of promoters.

The structure of the samples was characterized before and after their exposure in molten carbonate by scanning electron microscopy using a Hitachi S-2500 and X-ray diffraction using a SEIFERT 3000 P diffractometer with a Cu Kα radiation source. The chemical analyses of the samples were performed by ICP-AES (Jobin Yvon,JY-48/JY-38).

2.3. Electrochemical tests

The electrocatalytic activity of the cathode materials modified with rare earth oxides and the NiO taken as reference was studied by means of electrochemical impedance spectroscopy (EIS). The experimental cell (Fig. 1) used was described in our previous works [18,19]. These tests were carried out in the same experimental conditions than that of the stability tests: 62:38 Li:K eutectic melt, 650 °C and CO_2:O_2 4:1 and 200 h. The influence of gas composition was studied using atmospheres varying from 10 to 70% oxygen at constant

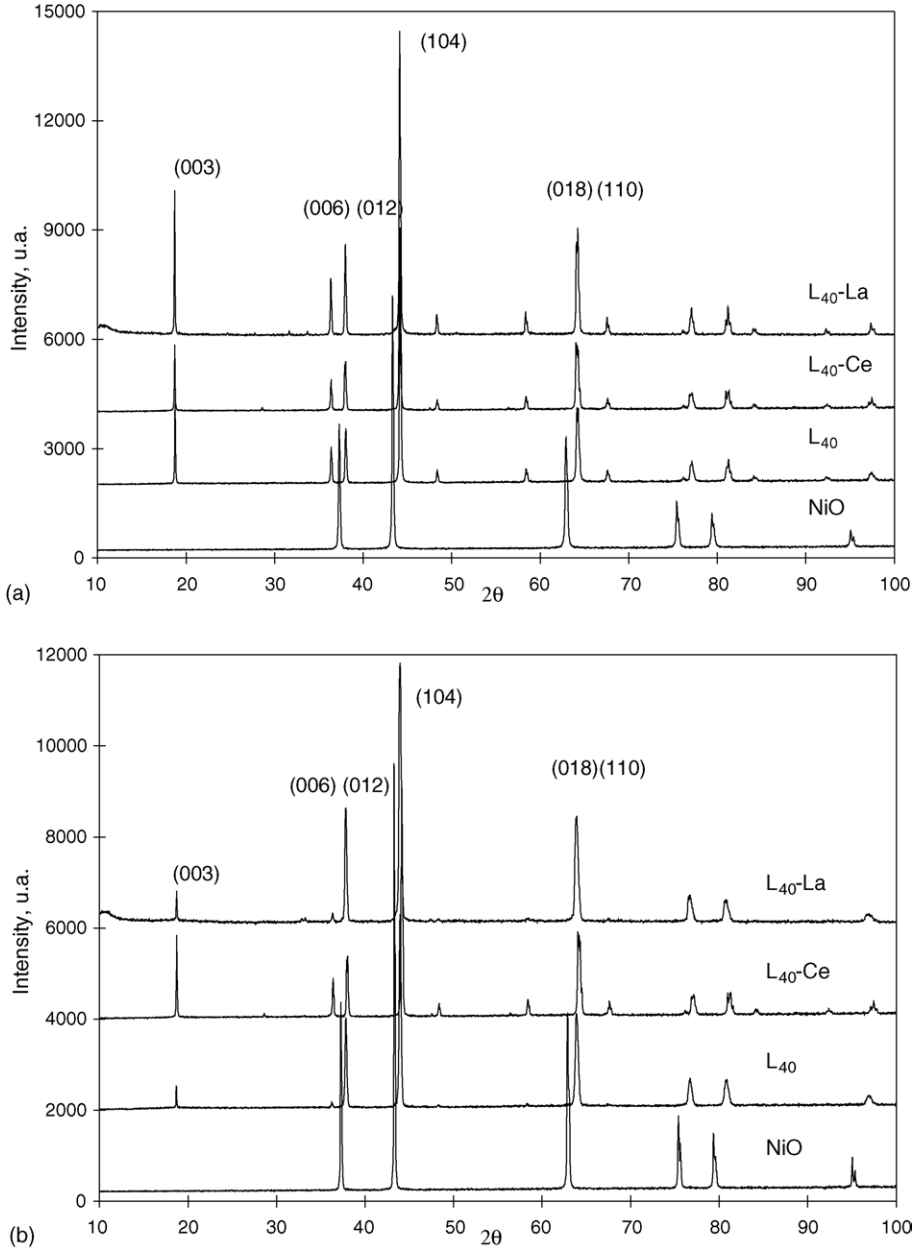

Fig. 2. XDR patterns of the lithium nickel mixed oxides prepared by solid-state reaction and NiO taken as reference before the immersion tests: (a) before exposure and (b) after exposure.

carbon dioxide content of 20% (balance N_2) and from 10 to 80% carbon dioxide with constant oxygen content of 10% (balance N_2).

The impedance spectra were recorded with a potentiostat/galvanostat (EG&G Model 263) and a Lock-in Amplifier (EG&G Model 5216). The amplitude of the sinusoidal voltage signal for the impedance measurements was 5 mV. The measurements were performed at five points per frequency decade between 100 kHz and 100 μHz at the open circuit potential. The impedance data were analyzed by using a modified transmission line model that was explained in a previous work [20].

3. Results and discussion

3.1. Stability tests

The concentrations of nickel dissolved into carbonate melt for the nickel oxide taken as reference and the three Li–Ni mixed oxides are given in the Table 1. For the lithium nickel mixed oxides, the concentrations of nickel measured in the carbonate melt were one order of magnitude lower than that of the NiO. The concentration of nickel for the samples modified with cerium (LNCe) or lanthanum (LNLa) was lower than LN. On the other hand, the content of lanthanum and cerium detected in the eutectic melt was 12 and 0.03 ppm, respectively. This result indicates a low dissolution of lanthanum and the stability of cerium in the molten carbonate. In general, similar morphology was observed for three lithium nickel mixed oxides before the stability test and higher particle size than for NiO. The presence of cerium or lanthanum did not affect to the morphology of the samples. Slight morphological changes were observed for the LN, LNCe and LNLa samples after the tests, while the nickel oxide suffered the growth of particles due to the lithiation process [21].

Table 1
Concentrations of Ni in the eutectic melt after the stability test

	Ni (ppm)
NiO	13.8
LN	3.3
LNCe	1.0
LNLa	2.4

The XRD patterns of all Li–Ni mixed oxides before and after their exposure showed the formation of $LiNiO_2$ rhombohedral structure as can be seen in Fig. 2. Initially, all Li–Ni mixed oxides showed the presence of peaks (0 0 3)

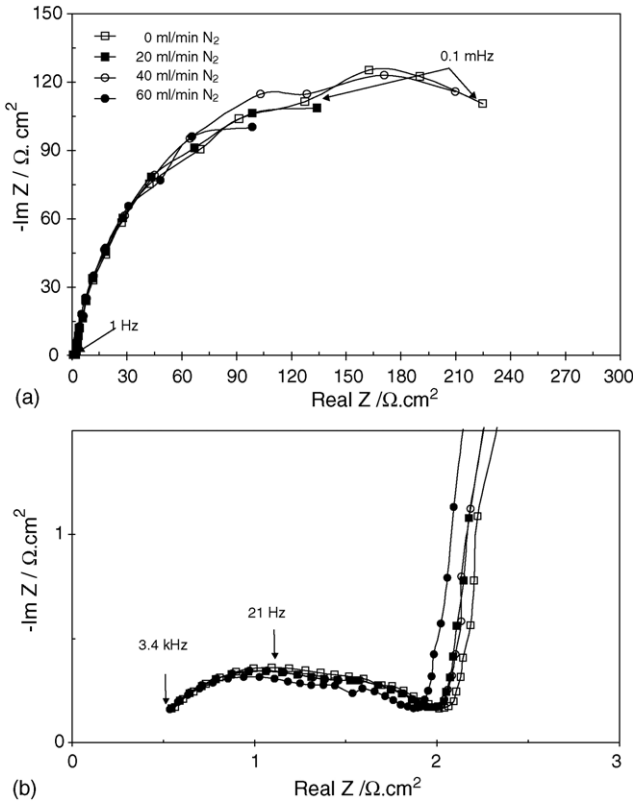

Fig. 3. The effect of introducing an inert gas (nitrogen) on the impedance spectra for LNCe at a flow constant of 10 ml min^{-1} O_2 and 40 ml min^{-1} CO_2: (a) low frequency region and (b) high frequency region.

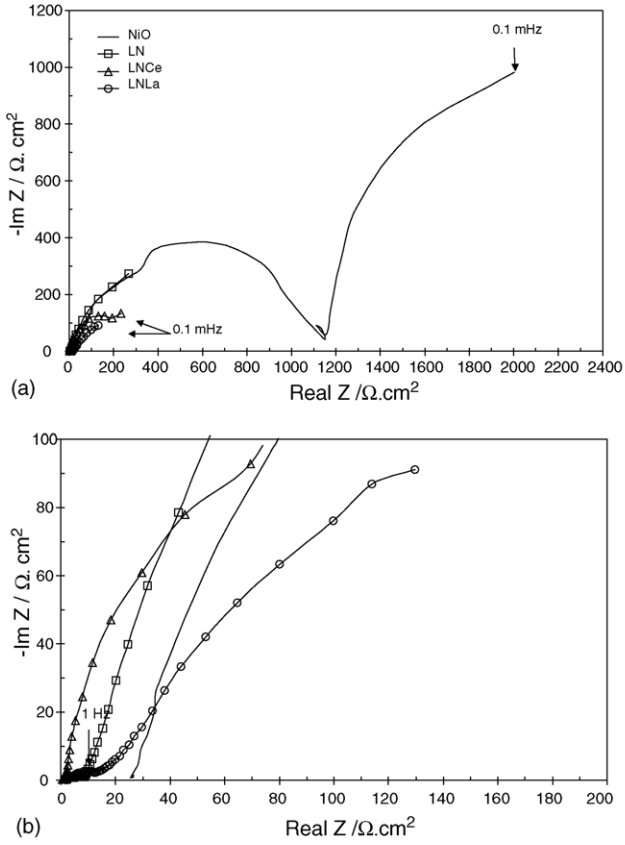

Fig. 4. Comparison of the impedance spectra of NiO, LN, LNCe and LNLa under an atmosphere of CO_2:O_2 (4:1) at 200 h: (a) low frequency region and (b) high frequency region.

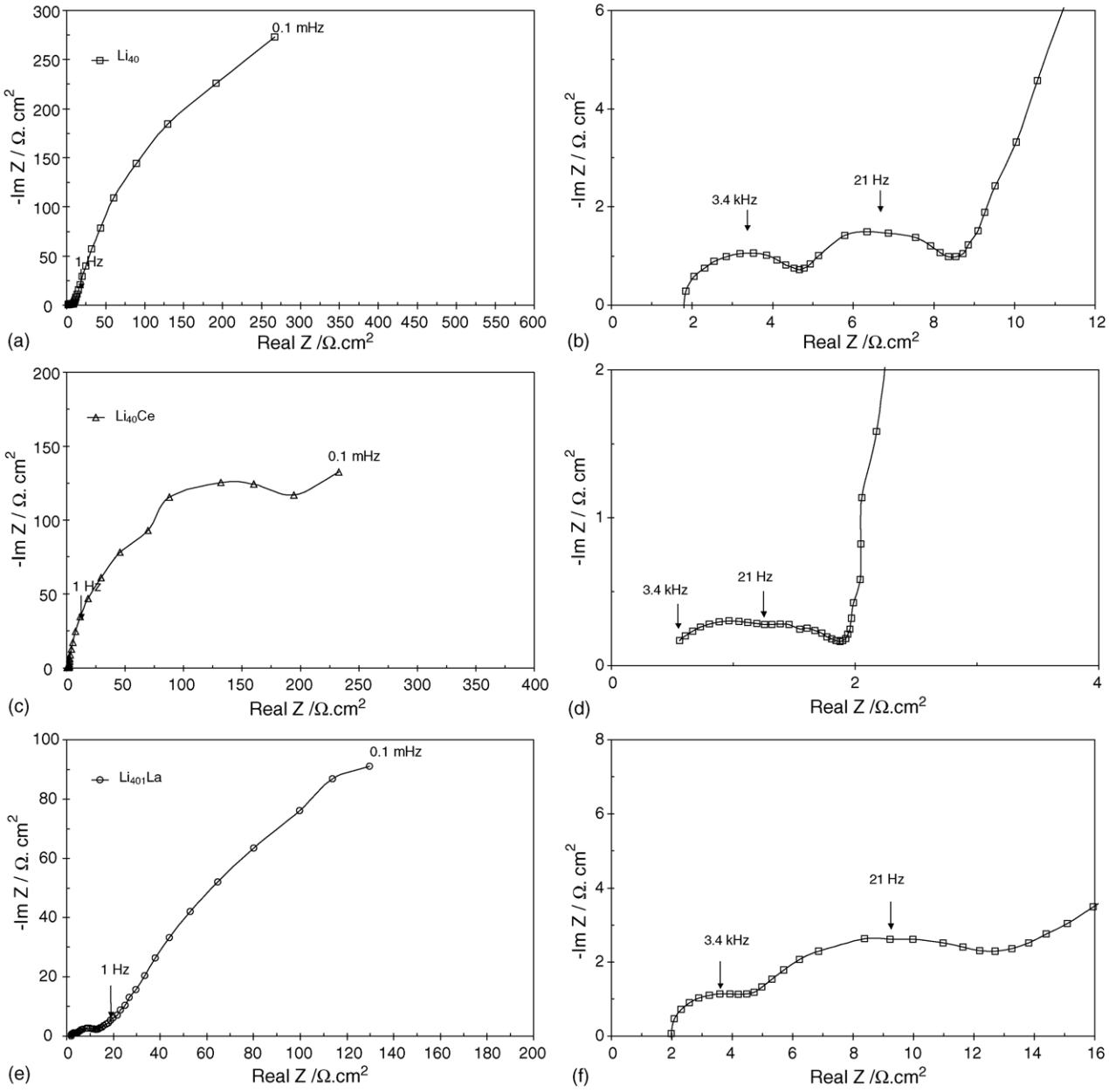

Fig. 5. Impedance spectra with a gas atmosphere of CO_2:O_2 4:1 at 200 h: (a) LN low frequency region; (b) LN high frequency region; (c) LNCe low frequency region; (d) LNCe high frequency region; (e) LNLa low frequency region and (f) LNLa high frequency region.

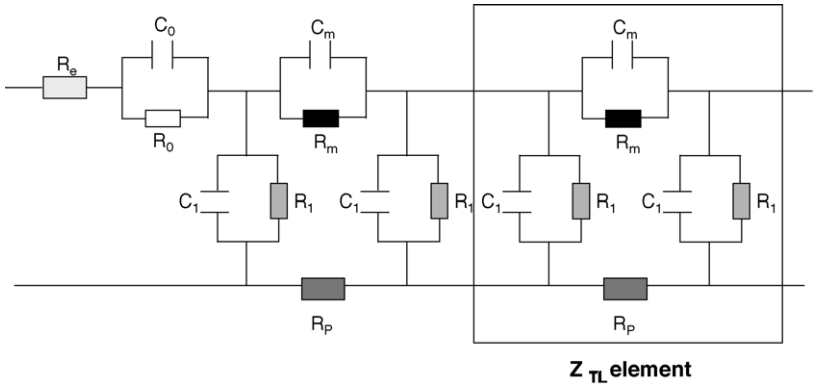

Fig. 6. Schematic representation of the transmission line used to fit the EIS data of the lithium nickel oxides.

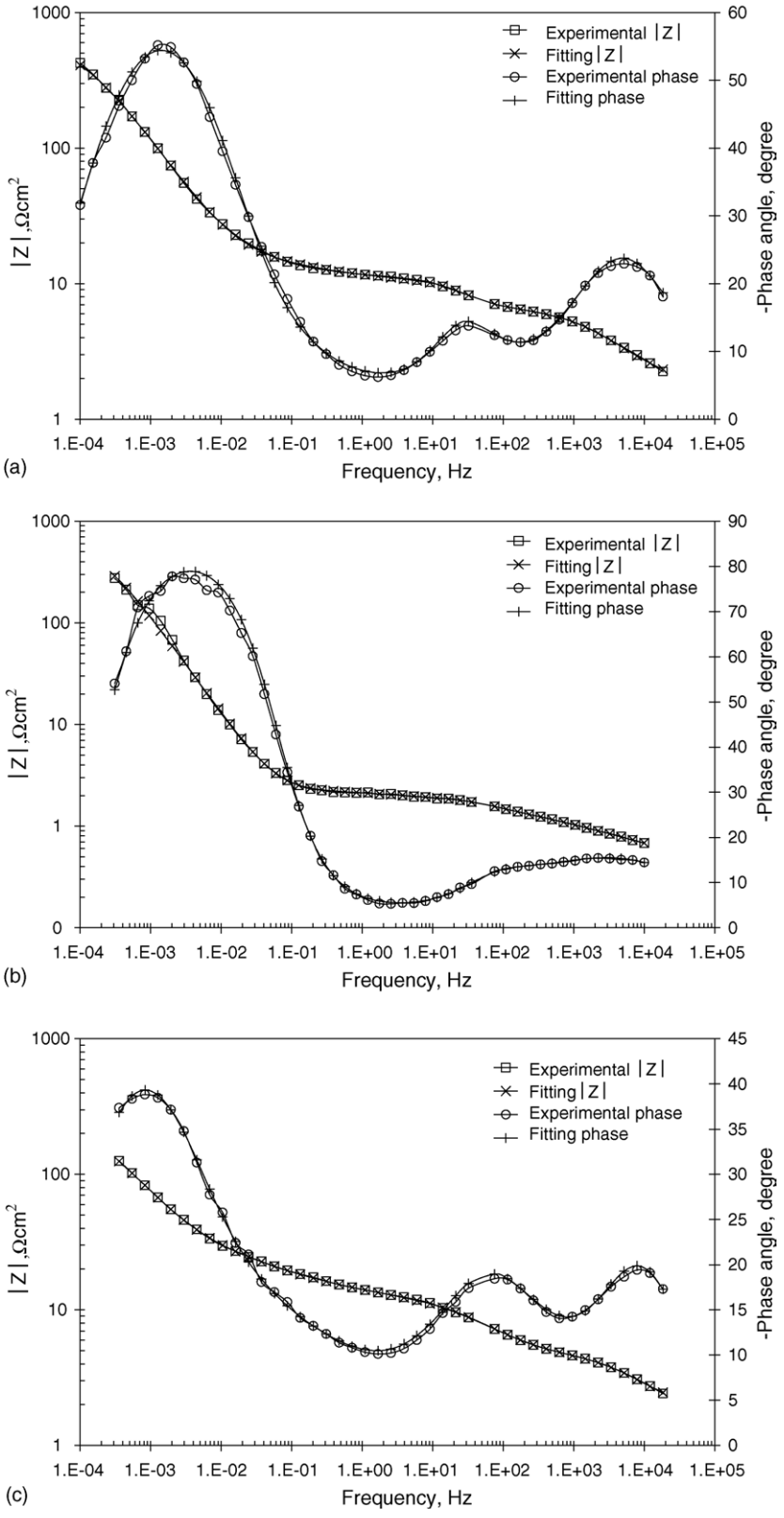

Fig. 7. Bode diagrams of the experimental and fitting data under an atmosphere of CO_2:O_2 (4:1) at 200 h: (a) LN; (b) LNCe and (c) LNLa.

and (1 0 4) peaks that reveal the formation of $LiNiO_2$ rhombohedral structure. It can be noted that after the exposure into the eutectic melt, the (0 0 3) peak presented a lower intensity being this line very sensitive to lithium amount (Fig. 2b). This result indicates that the lithium content in the oxide decreases because of the diffusions of lithium ions from the electrode to the eutectic melt. The cerium and the lanthanum could not be detected in the crystalline structure, due to very low content. Peaks corresponding to CeO_2 and La_2O_3 were only visible in the diffractograms for concentrations higher than 1 wt.% CeO_2 or La_2O_3.

3.2. Electrochemical tests

A comparative study by impedance spectroscopy of LN, LNCe, LNLa and NiO is presented in order to evaluate the effect of the addition of cerium oxide or lanthanum oxide in the electrocatalytic activity of the MCFC cathode for the reaction:

$$\tfrac{1}{2}O_2 + CO_2 + 2e^- \Leftrightarrow CO_3^{2-} \quad (1)$$

To determine that the electrochemical reduction of oxygen is whether or not a process controlled by the

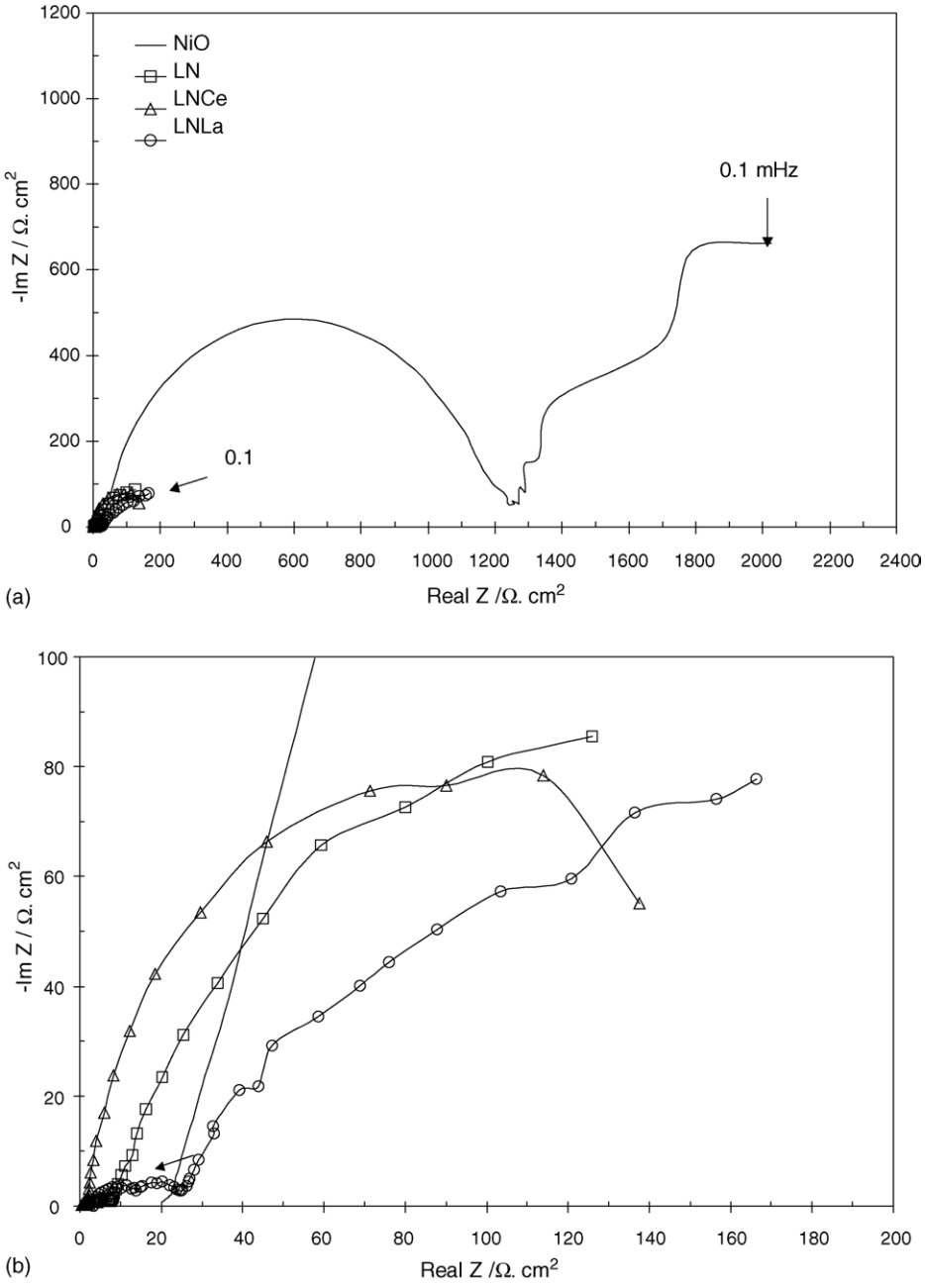

Fig. 8. Comparison of the impedance spectra of NiO, LN, LNCe and LNLa with a gas atmosphere of 70% O_2 and 20% CO_2: (a) low frequency region and (b) high frequency region.

diffusion, the effect of introducing an inert gas (nitrogen) from 0 to 60 ml min^{-1} with a constant flow of CO_2 (40 ml min^{-1}) and O_2 (10 ml min^{-1}) was studied with Li–Ni mixed oxides. As can be seen in Fig. 3, the impedance diagrams for LNCe are not appreciably influenced by variations of gas flow. This means that the reaction of oxygen reduction is not a diffusion-controlled process. Similar results were obtained by LN and LNLa.

A comparison of the Nyquist diagrams for the three lithium nickel mixed oxides (LN, LNCe and LNLa) and NiO taken as reference at 200 h is shown in Fig. 4. The lithium nickel mixed oxides showed impedance values lower by one-tenth than the nickel oxide by one-tenth, due to their higher conductivities. Therefore, the use of these novel materials as MCFC cathodes could reduce the ohmic loss causing an improve of the fuel cell performance.

Fig. 5 shows the impedance spectra for the LN, LNCe and LNLa at 200 h. All diagrams showed qualitatively the same features. As can be seen from the Nyquist plots, two

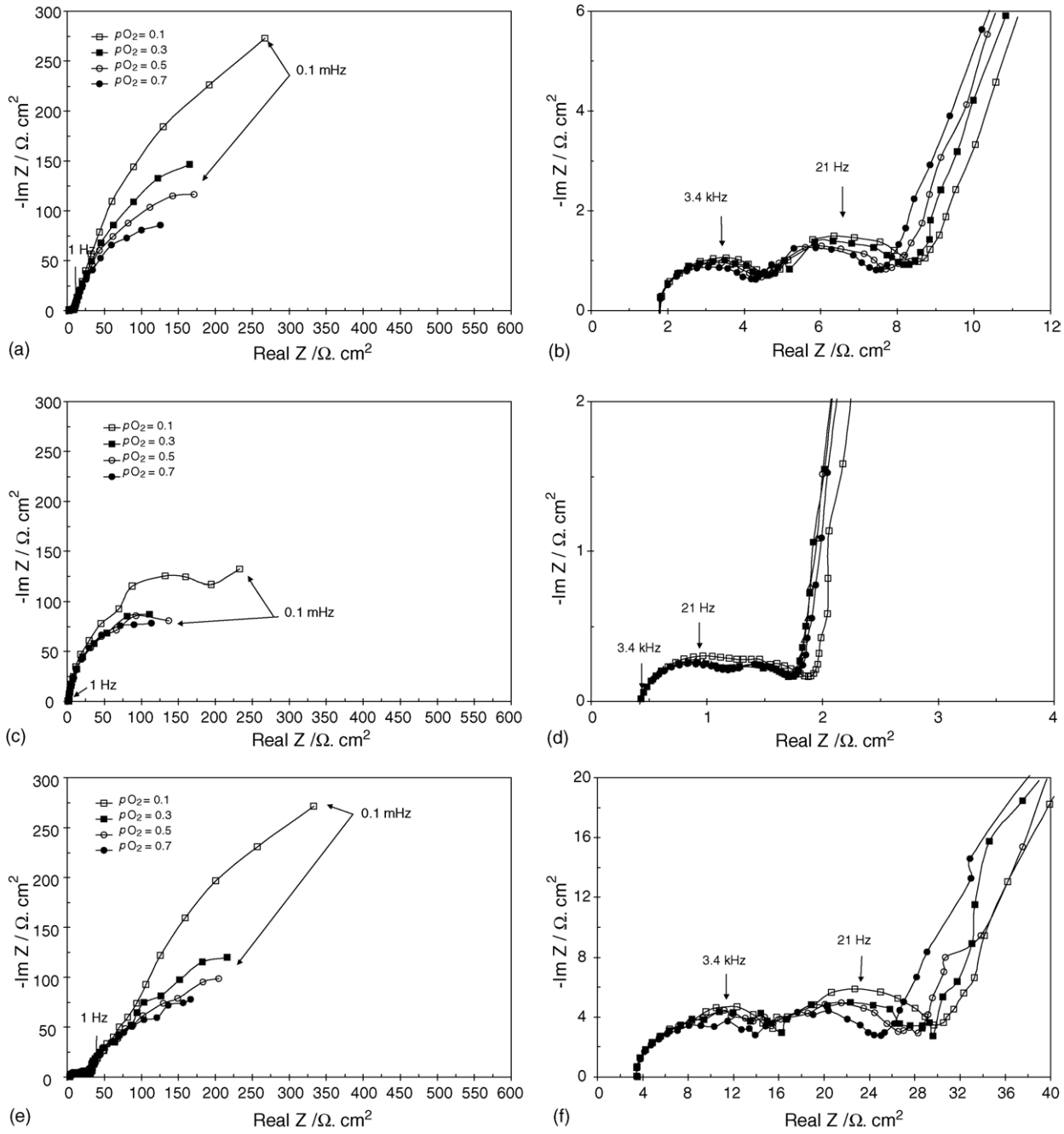

Fig. 9. Measured impedance spectra for Li–Ni mixed oxides at different O_2 contents of the gas with a constant CO_2 content of 20% (balance N_2): (a) LN low frequency region; (b) LN high frequency region; (c) LNCe low frequency region; (d) LNCe high frequency region; (e) LNLa low frequency region and (f) LNLa high frequency region.

well-differentiated regions are presented. In the high frequency region ($f > 1$ Hz) two arcs are observed.

The impedance spectra were interpreted using a modified transmission line model that includes contact impedance between particles that was explained in our previous work [20]. The impedance function, Z, is given by:

$$Z(\omega) = R_e + Z_0(\omega) + Z_{TL}(\omega) \quad (2)$$

where R_e corresponds to the electrolyte resistance and $Z_0(\omega)$ is the impedance associated to the inert volume of the electrode and the electrical contact. Z_{TL} represents the impedance for the reacting volume, schematically illustrated in Fig. 6. The corresponding expression can be written as:

$$Z_{TL}(\omega) = \frac{Z_m R_p L}{Z_m + R_p} + \frac{(Z_m^2 + R_p^2)\cosh(L\sqrt{\gamma}) + 2Z_m R_p}{(Z_m + R_p)\sqrt{\gamma}\sinh(L\sqrt{\gamma})} \quad (3)$$

where L is the effective length where the structural changes take place, $\gamma = (Z_m + R_p)/Z_1$ being Z_m the contact impedance along the transmission line and Z_1 the interfacial impedance that corresponds to the double layer capacitance in parallel with the charge-transfer processes including the oxygen reduction. R_p represents the electrolyte resistance along pores.

The intrinsic impedance, Z_0, the contact impedance, Z_m and the interface impedance, Z, can be expressed by the following general equation for a RC parallel association:

$$Z_i(\omega) = \frac{R_i}{1 + (j\omega R_i C_i)^{\alpha_i}} \quad (4)$$

where $j^2 = -1$. The parameter α_i is introduced to account for Cole–Cole type dispersion of the R_iC_i time constant. Details of the fitting procedure are given in Refs. [22,23].

In the high frequency region (Fig. 5b, d and f), two arcs are distinguished, the first one (at highest frequencies) associated with the intrinsic impedance of the non-reacting volume, and the second one related with the impedance of particle-to-particle contact. In case of the LNCe sample is more difficult to appreciate both arcs at high frequency due to a conjunction of the two arcs (Fig. 5d). The third arc in the low frequency region (Fig. 5a, c and e) corresponds to the charger-transfer processes associated with the oxygen reduction. So, the impedance of this arc is proportional to the resistance of transfer charger and a relative measure for the electrocatalytic activity. All experimental impedance data were fitted to Eq. (2), which corresponds to the circuit displayed in Fig. 6. In all cases, a good agreement exists between both experimental and simulated data in the whole frequency range as shown in Fig. 7.

Comparing the three Li–Ni oxides, the arc at low frequency (Fig. 5a, c and e) attributed to the resistance of transfer charger presented lower impedance values for the samples modified with rare earth oxides. This suggested that both cerium and lanthanum improve the charger-transfer processes associated with the oxygen reduction.

The impedance diagrams measured under a gas atmosphere rich in oxygen content ($pO_2 = 0.7$) for the three Li–Ni mixed oxides and NiO are shown in Fig. 8. The magnitude of impedance measured at high oxygen partial pressure for three Li–Ni mixed oxides appear to be similar and lower than for NiO. As discussed above this is most likely caused by the large specific resistivity of NiO compared to LN, LNCe and LNLa.

The dependence of oxygen partial pressure at constant $pCO_2 = 0.2$ for the three mixed oxides is presented in Fig. 9. The effect of oxygen content is more important in the low frequency arc (Fig. 9a, c and e). In the high frequency region, both arcs are not influenced by the oxygen content (Fig. 9b, d and f). For LN and LNLa, the low frequency arc decreases with increasing O_2 partial pressure. This suggests that the oxygen reduction reaction will be accelerated with the increase of pO_2. For LNCe, the processes of charge-transfer are not affected by the oxygen content from $pO_2 = 0.3$ to 0.7. This behavior can be attributed to cerium oxide acting as oxygen captor, supplying oxygen when it is necessary for the reaction of oxygen reduction.

This result may indicate that the addition of cerium oxide could be improved the electrocatalytic activity of the Li–Ni mixed oxides under gas atmosphere poor in oxygen.

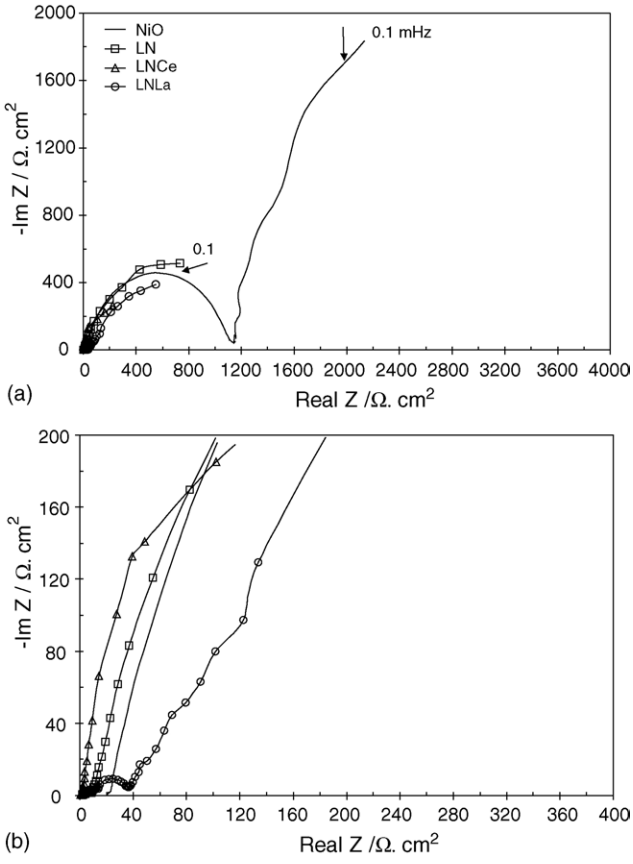

Fig. 10. Comparison of the impedance spectra of NiO, LN, LNCe and LNLa with a gas atmosphere of 10% O_2 and 70% CO_2: (a) low frequency region and (b) high frequency region.

Fig. 10 depicts the Nyquist plots measured under gas atmosphere rich in carbon dioxide (pCO_2), for the three samples and NiO. In these conditions, the impedances values of NiO are also one order of magnitude higher than the Li–Ni mixed oxides.

The effect of the carbon dioxide partial pressure at $pO_2 = 0.1$ atm for the three mixed oxides is shown in Fig. 11. For LN, the arc capacitive at low frequency increases with pCO_2, with a sudden rise at $pCO_2 = 0.8$ (Fig. 11a), while both arcs in the high frequency region, increase only at $pCO_2 = 0.8$ (Fig. 11b). This indicates that the process of charger-transfer is difficulted by the increase of carbon dioxide. For LNCe and LNLa, the low frequency arc increases slightly with pCO_2, but it is not a linear dependence (Fig. 11c and d). This may be due

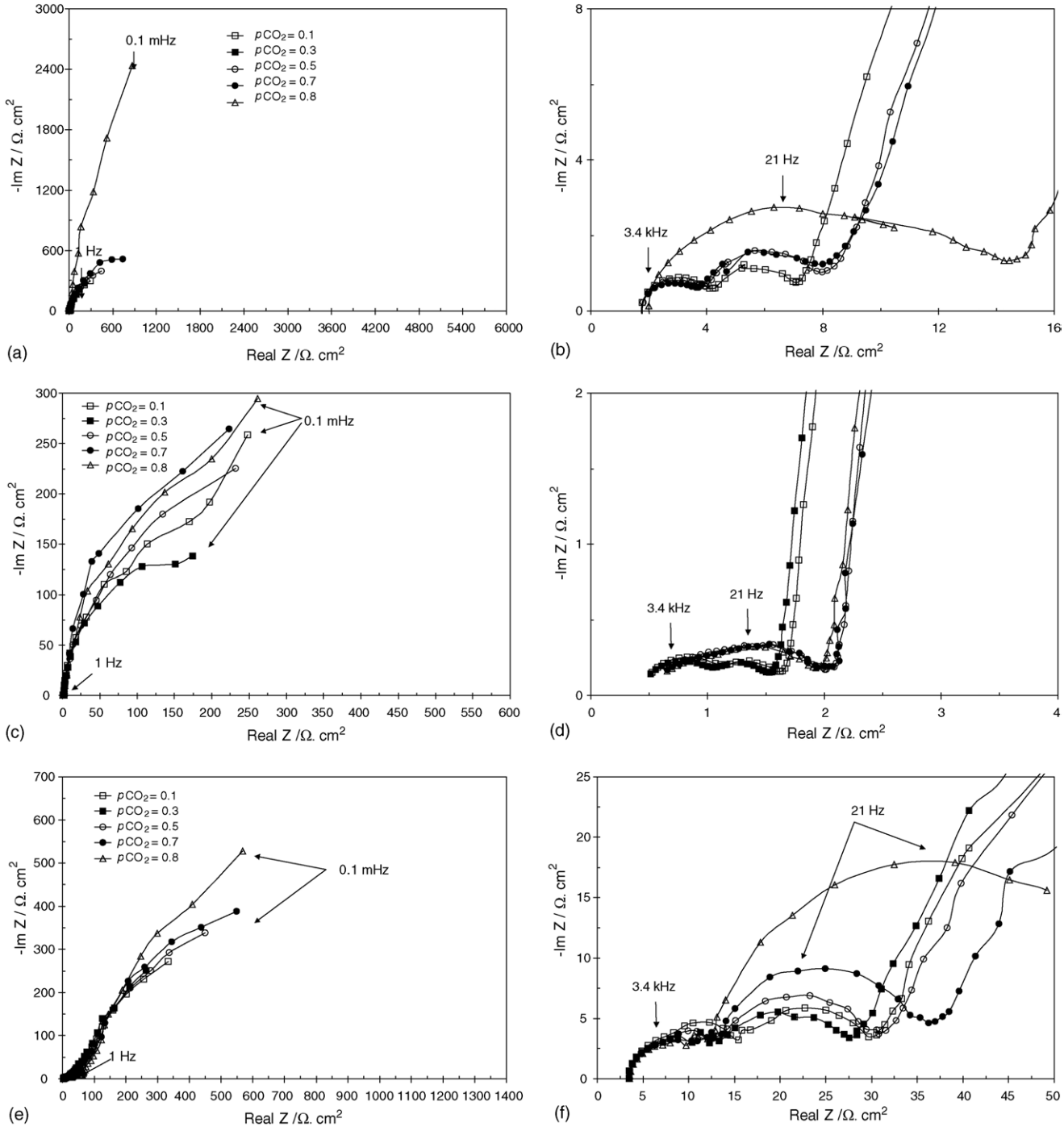

Fig. 11. Measured impedance spectra for Li–Ni mixed oxides at different CO_2 contents of the gas with a constant O_2 content of 10% (balance N_2): (a) LN low frequency region; (b) LN high frequency region; (c) LNCe low frequency region; (d) LNCe high frequency region; (e) LNLa low frequency region and (f) LNLa high frequency region.

to CeO_2 acting as oxygen buffer, and oxygen donor for the oxygen reduction reaction [24]. However, La_2O_3 captures CO_2 reducing the content of carbon dioxide on the surface of electrode due to the basic nature of La_2O_3. It is well known that CO_2 reacts with La_2O_3 and produces $La_2O_2CO_3$ species. This same behavior was observed by Tsipouri and Verykios [25]. In the high frequency region, only the second arc for LNLa depends on the partial pressure of CO_2 (Fig. 11e), indicating higher difficulty for the transport of oxygen to the reactive surface due to lanthanum.

Summing up, the influence of pCO_2 on LNCe and LNLa is lower than on LN sample (without promoters). This suggests that the addition of promoters as CeO_2 and La_2O_3 could improve the electrocatalytic activity for oxygen reduction reaction under gas atmosphere rich in carbon dioxide.

4. Conclusions

The dissolution of nickel for the Li–Ni mixed oxides is one order of magnitude lower than that of NiO. Samples with CeO_2 or La_2O_3 presented lower nickel dissolution than the Li–Ni oxides without promoters. CeO_2 is stable in the eutectic melt, while La_2O_3 suffered a low dissolution increasing the basicity of the electrolyte.

The incorporation of CeO_2 or La_2O_3 to the samples did not affect the morphology, while the NiO cathode suffered a strong recrystallization of particles. After 200 h of exposure in the eutectic melt under a gas atmosphere with high content of carbon dioxide, the morphology of Li–Ni mixed oxides did not show notable changes.

The reaction of oxygen reduction is not a diffusion-controlled process and the charger-transfer processes are accelerated by the increase of oxygen partial pressure and hindered by the increase of carbon dioxide partial pressure. The samples with CeO_2 or La_2O_3 showed lower resistance for charger-transfer processes than the sample without rare oxides. Both cerium and lanthanum improved the charger-transfer processes associated with the oxygen reduction. This could be due to CeO_2 acting as oxygen donor and La_2O_3 capturing carbon dioxide, reducing the carbon dioxide partial pressure on the surface of electrode. Therefore, the electrocatalytic activity of oxygen reduction reaction will increase, improving the fuel cell performance under an atmosphere rich in carbon dioxide.

References

[1] L. Giorgi, M. Carewska, S. Scaccia, E. Simoneti, E. Giacometti, R. Tulli, Int. J. Hydrogen Energy 21 (1996) 491.
[2] R.C. Makkus, K. Hemmes, J.H.W. de Wit, J. Electrochem. Soc. 141 (1994) 3429.
[3] L. Plomp, E.F. Sitters, C. Vessies, F.C. Eckes, J. Electrochem. Soc. 138 (1991) 629.
[4] A.P. Brown, G.H. Kucera, M.F. Roche, Fuel Cell Seminar, Tucson, Arizona, USA, Abstracts 29 November–2 December 1992, p. 125.
[5] T. Fukui, S. Ohara, H. Okawa, T. Hotta, M. Naito, J. Power Sources 86 (2000) 340.
[6] S.T. Kuk, Y.S. Song, S.I. Suh, J.Y. Kim, K. Kim, J. Mater. Chem. 11 (2001) 630.
[7] S.G. Kim, S.P. Yoon, J. Han, S.W. Nam, T.H. Lim, S.A. Hong, H.C. Lim, J. Power Sources 112 (2002) 109.
[8] J. Soler, T. González, M.J. Escudero, T. Rodrigo, L. Daza, J. Power Sources 106 (2002) 189.
[9] B. Fang, C. Zhou, X. Liu, S. Duan, J. Appl. Electrochem. 31 (2001) 201.
[10] F. Li, H.Y. Chen, Ch.M. Wang, K.A. Hu, J. Electroanal. Chem. 531 (2002) 53.
[11] C. Belhomme, E. Goyrba, M. Cassir, C. Tessier, J. Electroanal. Chem. 503 (2001) 69.
[12] K. Hatoh, J. Nikura, E. Yasumoto, T. Gamo, Denki Kagaku 64 (1996) 825.
[13] H.J. Choi, S.K. Ihm, T.H. Lim, S.A. Hong, J. Power Sources 61 (1996) 239.
[14] S. Mitsushima, K. Matsuzawa, N. Kamiya, K.I. Ota, Electrochim. Acta 47 (2002) 3823.
[15] L. Daza, C.M. Rangel, J. Baranda, M.T. Casais, M.J. Martínez, J.A. Alonso, J. Power Sources 86 (2000) 329.
[16] M.J. Escudero, X.R. Nóvoa, T. Rodrigo, L. Daza, J. Power Sources 106 (2002) 196.
[17] L. Daza, M.J. Escudero, E. Hontañón, C.M. Rangel, T. Rodrigo, M.T.Casais, M.J. Martínez, Fuel Cell Seminar, Portland, Oregon, USA, Abstracts 30 October–2 November 2000, p. 732.
[18] M.J. Escudero, Ph.D. Thesis, Universidad Autónoma de Madrid, Madrid, Spain, 2002.
[19] L. Giorgi, M. Carewska, S. Scaccia, E. Simoneti, E. Giacometti, R. Tulli, Int. J. Hydrogen Energy 21 (1996) 491.
[20] M.J. Escudero, X.R. Nóvoa, T. Rodrigo, L. Daza, J. Appl. Electrochem. 32 (2002) 929.
[21] M.J. Escudero, T. Rodrigo, J. Soler, L. Daza, J. Power Sources 118 (2003) 23.
[22] C.M. Abreu, M. Izquierdo, M. Keddam, X.R. Nóvoa, H. Takenouti, Electrochim. Acta 41 (1996) 2045.
[23] M. Keddam, H. Takenouti, X.R. Nóvoa, C. Andrade, C. Alonso, Cem. Conc. Res. 27 (1997) 1191.
[24] J. Baranda, Ph.D. Thesis, Universidad Autónoma de Madrid, Madrid, Spain, 1997.
[25] V.A. Tsipouriari, X.E. Verykios, Catal. Today 64 (2001) 83.